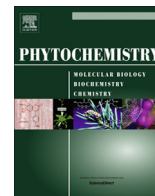




Contents lists available at ScienceDirect

Phytochemistry

journal homepage: www.elsevier.com/locate/phytochem

Galloylated flavonol rhamnosides from the leaves of *Calliandra tergemina* with antibacterial activity against methicillin-resistant *Staphylococcus aureus* (MRSA)

Elaine Wan Ling Chan^a, Alexander I. Gray^b, John O. Igoli^b, Sui Mae Lee^a, Joo Kheng Goh^{a,*}

^aSchool of Science, Monash University Malaysia, Jalan Lagoon Selatan, 46150 Bandar Sunway, Selangor, Malaysia

^bStrathclyde Institute of Pharmacy and Biomedical Sciences, University of Strathclyde, John Arbuthnott Building, 161 Cathedral Street, Glasgow G4 0RE, United Kingdom

ARTICLE INFO

Article history:

Received 29 October 2013

Received in revised form 18 July 2014

Available online xxxx

Keywords:

Calliandra tergemina

Leguminosae

Flavonol rhamnosides

Antimicrobial

Methicillin-resistant *Staphylococcus aureus*

ABSTRACT

Galloylated flavonol rhamnosides identified as kaempferol-3-*O*-(2'',3'',4''-tri-*O*-galloyl)- α -L-rhamnopyranoside, quercetin-3-*O*-(3'',4''-di-*O*-galloyl)- α -L-rhamnopyranoside, and quercetin-3-*O*-(2'',3'',4''-tri-*O*-galloyl)- α -L-rhamnopyranoside, together with five known galloylated and non-galloylated flavonol rhamnosides, were isolated from leaves of *Calliandra tergemina* (L.) Benth. Their structures were established using spectroscopic methods and their antibacterial activities against methicillin-resistant *Staphylococcus aureus* (MRSA) were evaluated by a microdilution method.

© 2014 Elsevier Ltd. All rights reserved.

1. Introduction

The genus *Calliandra* belongs to the family Leguminosae and subfamily Mimosaceae. The family has about 200 species of flowering plants native to tropical America, Madagascar and India. Several species are planted as ornamental plants (Mattagajasingh et al., 2006). There is, however, presently no paper describing the chemical constituents and bioactivity of *Calliandra tergemina* although there are reports on several related species including *Calliandra portoricensis*, *Calliandra californica* and *Calliandra haematocephala* (Aguwa and Lawal, 1988; Encarnacion et al., 1994; Agunu et al., 2005; Moharram et al., 2006; Orishadipe et al., 2010). Preliminary screening of the leaf extracts of *C. tergemina* displayed antibacterial activity against *Micrococcus luteus*, *Bacillus cereus*, methicillin-sensitive *Staphylococcus aureus* (MSSA) and methicillin-resistant *Staphylococcus aureus* (MRSA), respectively (Chew et al., 2011). The activity against MRSA is interesting as the latter is a major cause of infections in hospitals and resistant to all known β -lactam antibiotics (Otsuka et al., 2008; Chew et al., 2011). Thus a bioassay-guided fractionation of *C. tergemina* leaf extracts, coupled with chromatographic separation, was employed to isolate the active constituents. This yielded three new galloylated flavonol rhamnosides and five known flavonol rhamnosides.

This paper describes the isolation, structure elucidation and the structure–activity relationships of the isolated compounds.

2. Results and discussion

Five crude extracts were obtained from the leaves of *C. tergemina* of which the ethyl acetate extract had the highest anti-MRSA activity (Table 1); and from his extract, eight flavonol glycosides were isolated using a combination of silica gel column and gel filtration chromatography. Three new compounds were identified by their NMR (¹H, ¹³C, HSQC, HMBC), UV and mass spectra, optical rotations, and by comparison with previously reported spectroscopic data. The five known galloylated and non-galloylated flavonol rhamnosides were quercetin-3-*O*-(3''-*O*-galloyl)- α -L-rhamnopyranoside (4) (Moharram et al., 2006), quercetin-3-*O*- α -L-rhamnopyranoside (5) (Eldahshan, 2011), kaempferol-3-*O*-(2'',3''-di-*O*-galloyl)- α -L-rhamnopyranoside (6) (Lee et al., 2009), kaempferol-3-*O*-(3''-*O*-galloyl)- α -L-rhamnopyranoside (7) (Mahmoud et al., 2001) and kaempferol-3-*O*- α -L-rhamnopyranoside (8) (Eldahshan, 2011); respectively.

Kaempferol-3-*O*-(2'',3'',4''-tri-*O*-galloyl)- α -L-rhamnopyranoside (1), quercetin-3-*O*-(3'',4''-di-*O*-galloyl)- α -L-rhamnopyranoside (2) and quercetin-3-*O*-(2'',3'',4''-tri-*O*-galloyl)- α -L-rhamnopyranoside (3) are new and their 1D and 2D NMR and HRESIMS spectra are provided as Supporting information (Figs. S1–S3).

* Corresponding author. Tel.: +60 3 5514 6108; fax: +60 3 5514 6364.

E-mail address: goh.joo.kheng@monash.edu (J.K. Goh).

Table 1
Antimicrobial activity of different solvent extracts of *C. tergemina* leaves.

Extract/control	Diameter of zone of inhibition (mm)		
	MRSA ATCC (33591)	MRSA (Clinical Isolate 1)	MRSA (Clinical Isolate 2)
Vancomycin	21.0 ± 0.0	20.2 ± 0.3	18.5 ± 0.5
Hexane	nd ^a	nd ^a	nd ^a
Dichloromethane	nd ^a	nd ^a	nd ^a
Ethyl Acetate	15.2 ± 0.3	13.0 ± 0.0	11.2 ± 0.3
Methanol	13.0 ± 0.0	11.0 ± 0.0	10.5 ± 0.5
Water	nd ^a	nd ^a	nd ^a

Vancomycin (0.030 mg/disc); Plant extract (1 mg/100 µl per disc). Values are the means of three replicates ± SD.

^a (nd) non-detectable.

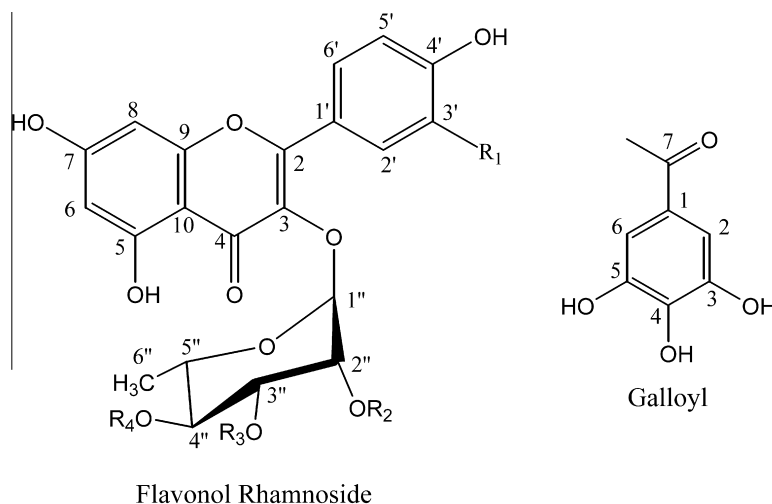
2.1. Structural elucidation of 1–3

Compound **1**, kaempferol-3-*O*-(2'',3'',4''-tri-*O*-galloyl)- α -L-rhamnopyranoside, was obtained as a yellow amorphous powder. Its Q-TOFMS gave a molecular ion at m/z 887.1322 for $[M-H]^-$, supporting a molecular formula of $C_{42}H_{32}O_{22}$. In the 1H NMR spectrum of **1** (Table 3 and S1), two doublets with *meta* couplings were observed at δ_H 6.31 (H-6) and δ_H 6.53 (H-8) for the 5,7-dihydroxy A-ring, and two aromatic doublets characteristic of a 1,4-disubstituted benzene ring at δ_H 7.22 (H-3'/H-5') and δ_H 8.03 (H-2'/H-6') also suggested the flavonol moiety was kaempferol. A proton singlet due to an -OH group at C-5, chelated to the carbonyl at C-4, was also observed at δ_H 12.57 ppm. In the HMBC spectrum, this latter proton correlated with C-5, C-6 and C-10. In the carbohydrate region, there were signals for a secondary methyl doublet at δ_H 0.99 (3H, d, H-6''), an anomeric proton at δ_H 5.97 (d, H-1'') and four oxygen-bearing methines at δ_H 5.98 (dd, H-2''), 5.70 (dd, H-3''), 5.42 (t, H-4''), and 3.71 (dq, H-5''). These data suggested that compound **1** was a kaempferol rhamnoside derivative. The 1H NMR spectrum of **1** was also similar to that of kaempferol-3-*O*- α -L-rhamnopyranoside (**8**) and kaempferol-3-*O*-(2'',3''-di-*O*-galloyl)- α -L-rhamnopyranoside (**6**), (Lee et al., 2009; Eldahshan, 2011), except for one additional galloyl moiety. The rhamnose H-1'' proton of **1** showed a weak correlation to a carbon at 133.7 ppm (C-3) in a similar fashion to that shown in the HMBC spectrum for compound **8**. The galloylation of the rhamnosyl group in **1** was evident from the three sets of galloyl protons appearing as two-proton singlets at δ_H 6.98, 7.01 and 7.17 ppm. The positions of substitution of the galloyl groups were determined by analysis of the downfield shifts of the sugar protons: H-2'' (δ_H 5.98), H-3'' (δ_H 5.70) and H-4'' (δ_H 5.42) compared to **8** with no galloyl groups (δ_H 3.47, 3.97, 3.08), **7** with a galloyl group at C-3'' (δ_H 4.56, 5.24, 3.79), and **6** with two galloyl groups at C-2'' and C-3'' (δ_H 5.94, 5.50, 3.83), respectively. Similar down-field shifts of the rhamnosyl protons have been reported for kaempferol-3-*O*-(2'',3'',4''-tri-*O*-acetyl-rhamnopyranoside (Usia et al., 2004). In its ^{13}C NMR spectrum, three carbonyl carbons from the galloyl groups were observed at δ_C 164.5, 164.9 and 165.2 ppm, with the methyl carbon of the rhamnosyl moiety (C-6'') being at δ_C 16.9 ppm. In the 1H - 1H ASANOESY spectrum, the methyl protons (H-6'', δ_H 0.99) correlated with H-5'' (δ_H 3.71) and H-4'' (δ_H 5.41). That the latter two protons were axial was deduced by the large coupling constant ($J = 10.0$ Hz) and H-3'' had the same coupling constant with H-4'' indicating that it was also axial, while H-2'' must be equatorial as the coupling constant to H-3'' was small ($J = 3.1$ Hz). H-3'' and H-5'' had strong NOE interactions with one another indicative of their 1,3-diaxial orientation. The rhamnosyl anomeric proton (H-1'', δ_H 5.97, $J = 1.8$ Hz) did not have any detectable NOE interactions with H-3'' nor H-5'' showing that these three protons were not on the same

face of the sugar; i.e. H-1'' did not have a 1,3-diaxial relationship with H-3'' and H-5''. Therefore, H-1'' must be equatorial and on the opposite side of the sugar from H-3'' and H-5'' as in α -L-rhamnosides. The NOESY experiment also exhibited correlations between the sugar protons (H-1'', 2'' and 3'') and the aromatic protons H-2'/6' giving further proof of the rhamnosyl attachment in C-3. The absolute configuration of the rhamnose was determined to be L-based on the optical rotation after acid hydrolysis of compound **1**. Thus, compound **1** was identified as kaempferol-3-*O*-(2'',3'',4''-tri-*O*-galloyl)- α -L-rhamnopyranoside. The complete assignment of the 1H and ^{13}C NMR resonances was made possible by analysis of its HMBC and HSQC spectra (S1).

Compound **2**, quercetin-3-*O*-(3'',4''-di-*O*-galloyl)- α -L-rhamnopyranoside, was also obtained as a yellow amorphous powder. Its Q-TOFMS gave a molecular ion peak at m/z 751.1156 for $[M-H]^-$ attributed to a molecular formula of $C_{35}H_{28}O_{19}$. The 1H NMR spectroscopic data of compound **2** (Table 3 and S2) showed the presence of an ABX-type aromatic system, this being characteristic of a 3',4'-disubstituted B-ring of a flavone with the ring protons at H-2' (δ_H 7.61, d, $J = 2.1$ Hz), H-6' (δ_H 7.50, dd, $J = 8.3, 2.1$ Hz) and H-5' (δ_H 7.14, d, $J = 8.3$ Hz), respectively. Two doublets with *meta* couplings at δ_H 6.31 (1H, d, $J = 2.1$ Hz) and 6.52 (1H, d, $J = 2.1$ Hz) were observed for the H-6 and H-8 of the 5,7-dihydroxy substituted ring A of the flavonol moiety. The carbohydrate proton region was similar to that of compound **1**, and there were also resonances for a secondary methyl signal at δ_H 0.88 (3H, d, H-6''), an anomeric proton at δ_H 5.78 (d, H-1'') and four oxygen-bearing methines at δ_H 4.62 (br dd, H-2''), whose position is shielded compared to that of H-2'' in **1**, 5.46 (dd, H-3''), 5.41 (t, H-4'') and 3.62 (dq, H-5''), respectively. This indicated that compound **2** was a quercetin derivative. The presence of two galloyl moieties in compound **2** was inferred from the two-proton singlets observed in the aromatic region of its 1H NMR spectrum due to H-2''' and H-6''' of the galloyl groups. These resonances were similar to the 1H NMR spectroscopic data for quercetin 3''-*O*-galloyl-rhamnopyranoside and quercetin 2'',3''-di-*O*-galloyl-rhamnopyranoside (Moharram et al., 2006; Eldahshan, 2011), except for the position of the galloyl groups. The positions of the galloyl groups in compound **2** were determined to be at C-3'' and C-4'' on the basis of the down-field shift of H-3'' ($\delta_H = 5.46$) and H-4'' ($\delta_H = 5.41$) compared to compound **5** with no galloyl groups ($\delta_H = 3.51, 3.20$) and compound **4** with a galloyl group at C-3'' ($\delta_H = 5.27, 3.80$), respectively. The ^{13}C NMR spectrum was similar to that of compound **1**; the carbonyl signals at 165.0 and 165.5 were assigned to the two galloyl groups and the methyl carbon for the rhamnosyl group (C-6'') was observed at 16.8 ppm. Similarly, the small J value (1.8 Hz) of the anomeric proton at δ_H 5.78 in compound **2** and correlations in its 2D NMR spectra similar to **1** also indicated the α -configuration for the rhamnosyl moiety. Compound **2** was thus identified as quercetin-3-*O*-(3'',4''-di-*O*-galloyl)- α -L-rhamnopyranoside.

Compound **3**, quercetin-3-*O*-(2'',3'',4''-tri-*O*-galloyl)- α -L-rhamnopyranoside, was similarly obtained as a yellow amorphous powder. Its molecular formula was determined to be $C_{42}H_{32}O_{23}$, based on its Q-TOFMS, which gave a molecular ion peak at m/z 903.1264 $[M-H]^-$. The 1H NMR, ^{13}C NMR, COSY, HSQC and HMBC spectra of compound **3** were similar to those of compound **2** except for an additional galloyl group in compound **3**. The 1H NMR spectrum showed three aromatic singlets for three galloyl groups at 7.16, 7.03 and 6.98 ppm. The positions of attachment of the galloyl groups in compound **3** were deduced as for compound **1** which showed very similar downfield shifts of H-2'' (δ_H 5.99), H-3'' (δ_H 5.66) and H-4'' (δ_H 5.41). This was further confirmed by analysis of its ^{13}C NMR spectrum with three carbonyl carbons for the galloyl groups at δ_C 164.6, 164.9 and 165.3 ppm; the 2D NMR correlations, as well as chemical shifts for the flavonoid nucleus, were also almost identical with that of **2** while those of the sugar mirrored



	R ₁	R ₂	R ₃	R ₄		R ₁	R ₂	R ₃	R ₄
1	H	Galloyl	Galloyl	Galloyl	5	OH	H	H	H
2	OH	H	Galloyl	Galloyl	6	H	Galloyl	Galloyl	OH
3	OH	Galloyl	Galloyl	Galloyl	7	H	H	Galloyl	H
4	OH	H	Galloyl	H	8	H	H	H	H

Fig. 1. Structures of isolated compounds 1–8.

those of **1**. Thus compound **3** was identified as quercetin-3-*O*-(2'',3'',4''-tri-*O*-galloyl)- α -L-rhamnopyranoside (Fig. 1).

2.2. Biological evaluation

2.2.1. Antibacterial activity against MRSA

Compounds **1**, **2**, **3** and **6** with multiple galloyl groups showed weak antibacterial activity against three strains of MRSA at 256 μ g/mL (Table 2). There was no detectable anti-MRSA activity for the compounds without galloyl groups or with a single galloyl group. These results were consistent with those reported for kaempferol and quercetin rhamnosides with *para*-coumaric acid esters (Otsuka et al., 2008). Antibacterial activities were observed for the acetylated rhamnosides, but not for the non-acylated kaempferol or quercetin rhamnosides (Otsuka et al., 2008). However, flavonol with acylated coumaroyl groups seem to possess more potent antibacterial activity against MRSA than flavonol with acylated galloyl groups. In addition, the degree of esterification was not directly correlated to the antibacterial activity as the compounds with two and three galloyl groups had the same minimum inhibitory concentration (MIC). This is in contrast to the report that

the antioxidant activity of galloylated flavonol rhamnosides has a direct correlation with the number of galloyl groups (Moharram et al., 2006). The results obtained here, however, showed that esterification of the rhamnoside moiety was more important in conferring anti-MRSA activity than the corresponding flavonol rhamnoside and there was no correlation between anti-MRSA activity and the degree of esterification. Antibacterial activity for the flavonol rhamnosides could be increased by multiple esterification of the rhamnoside moiety. Although the anti-MRSA activity of the isolated compounds was low, these flavonol rhamnosides might be able to reverse the susceptibility of MRSA towards β -lactam antibiotics when used in combination as flavonoids with a low antibacterial activity have been found to intensify the susceptibility of MRSA towards β -lactam antibiotics at a concentration much lower than the MIC (Sato et al., 2004).

2.2.2. Effects of flavonol rhamnosides on MRSA cells

The morphological changes of MRSA cells after treatment with *C. tergemina* leaf extracts and the flavonol rhamnosides were observed under a scanning electron microscope (SEM) to determine the mode of action of the flavonol rhamnosides on MRSA

Table 2

Minimum inhibition concentrations (MICs) of flavonol rhamnosides from *C. tergemina*.

Compounds/Extracts	Number of galloyl groups	Minimum inhibition concentration (μ g/mL)		
		MRSA ATCC (33591)	MRSA (Clinical Isolate 1)	MRSA (Clinical Isolate 2)
Vancomycin (control)		4	4	4
Ethyl acetate extract		512	512	512
1	3	256	256	256
2	2	256	256	256
3	3	256	256	256
4	1	>1000	>1000	>1000
5	0	>1000	>1000	>1000
6	2	256	256	256
7	1	>1000	>1000	>1000
8	0	>1000	>1000	>1000

Compound **1**, **6**, **7** and **8** were kaempferol rhamnoside derivatives while compound **2**, **3**, **4** and **5** were quercetin rhamnoside derivatives.

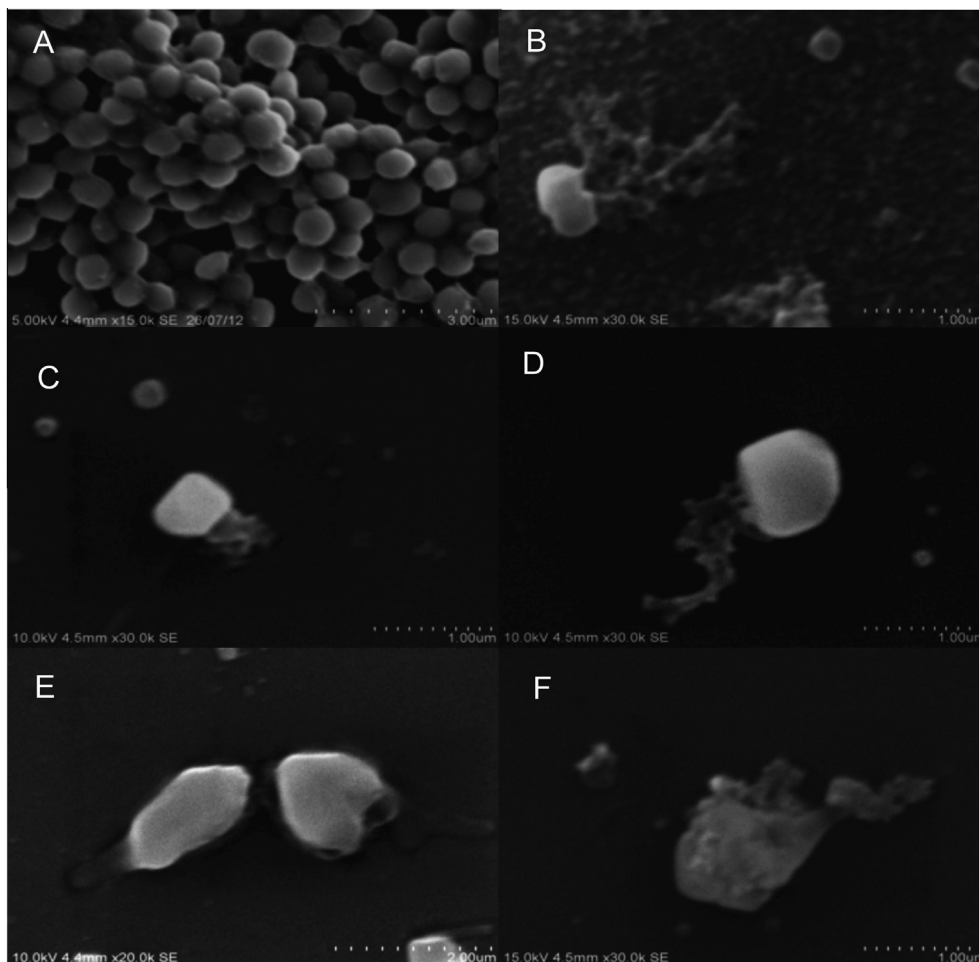


Fig. 2. Scanning electron microscope (SEM) photograph of MRSA treated with ethyl acetate leaf extracts and isolated active compounds of *C. tergemina* at 512 $\mu\text{g}/\text{mL}$ ($2\times$ MICs). (A) Control; (B) treated with ethyl acetate leaf extracts; kaempferol derivatives: (C) treated with compound **1**; (D) treated with compound **6**; quercetin derivatives: (E) treated with compound **2**; (F) treated with compound **3**.

Table 3
 ^1H NMR spectroscopic data of **1–3** in $(\text{CD}_3)_2\text{CO}$ at 400 MHz. δ_{H} in ppm and (*J* values in Hz).

Moiety	Position	1	2	3
Kaempferol/ Quercetin	6	6.31 (d, 2.1)	6.31 (d, 2.1)	6.30 (d, 2.1)
	8	6.53 (d, 2.1)	6.52 (d, 2.1)	6.52 (d, 2.1)
	2'/6'	8.03 (d, 8.8)	–	–
	2'	–	7.61 (d, 2.1)	7.64 (d, 2.1)
	3'/5'	7.22 (d, 8.8)	–	–
	5'	–	7.14 (d, 8.4)	7.18 (d, 8.4)
Rhamnose	6'	–	7.50 (dd, 8.4, 2.1)	7.55 (dd, 8.4, 2.1)
	OH (C-5)	12.57 (s)	12.68 (s)	12.58 (s)
	1''	5.97 (d, 1.8)	5.78 (d, 1.8)	5.97 (d, 1.9)
	2''	5.98 (dd, 3.1, 1.8)	4.62 (br dd, 2.8, 1.8)	5.99 (dd, 3.2, 1.9)
	3''	5.70 (dd, 10.0, 3.1)	5.46 (dd, 10.1, 2.8)	5.66 (dd, 10.1, 3.2)
	4''	5.42 (t, 10.0)	5.41 (t, 10.1)	5.41 (t, 10.1)
Galloyl A	5''	3.71 (dq, 10.0, 6.2)	3.62 (dq, 10.1, 6.3)	3.67 (dq, 10.1, 6.2)
	6''	0.99 (d, 6.2)	0.88 (d, 6.3)	0.97 (d, 6.2)
	2'''/6'''	7.17 (s)	7.04 (s)	7.16 (s)
Galloyl B	2'''/6'''	7.01 (s)	7.07 (s)	7.03 (s)
Galloyl C	2'''/6'''	6.98 (s)	–	6.98 (s)

cells. In the control cells, the MRSA cells appeared as grape-like clusters (Fig. 2A). After treating the MRSA cells with 512 $\mu\text{g}/\text{mL}$ ($2\times$ MICs) of the ethyl acetate extract and isolated compounds **1**, **2**, **3** and **6**, the grape-shaped cluster of MRSA cells were disrupted and the remaining cells showed leakage of cellular contents (Fig. 2C–F). There were no differences in the antibacterial effects on the MRSA cells between the quercetin and kaempferol rhamnosides. The compounds all caused cellular leakage of MRSA cells.

Phenolic compounds are reported to act specifically on the bacterial membrane and cause bacterial cell leakage (Johnston et al., 2003; Nohynek et al., 2006). Polyphenols in tea such as epicatechin and gallic acid have been shown to cause leakage of cellular contents in *Lactobacillus plantarum* and *Neisseria meningitidis* (Cho et al., 2010). This leakage can be clearly observed in Fig. 2C, when MRSA cells were treated with compound **1**. Phenolic compounds, such as these flavonol rhamnosides, are able to cause

Table 4
¹³C NMR data of compounds 1–3.

Moiety	Position	1	2	3
Kaempferol/quercetin	2	157.2	157.7	157.9
	3	133.7	134.2	133.0
	4	178.0	178.3	178.0
	5	162.4	162.3	162.4
	6	98.9	99.0	98.9
	7	164.3	164.2	164.3
	8	93.9	93.8	94.0
	9	157.7	157.2	157.2
	10	104.9	104.9	104.9
	1'	121.7	122.2	122.0
Rhamnose	2'	131.0	116.1	116.1
	3'	116.0	145.2	145.3
	4'	159.8	148.0	148.1
	5'	116.0	115.8	115.9
	6'	131.0	121.9	122.1
	1''	98.0	100.8	97.8
	2''	69.3	68.2	69.1
	3''	69.5	72.1	69.7
	4''	70.4	70.3	70.3
	5''	68.7	68.4	68.6
Galloyl A	6''	16.9	16.8	16.9
	1'''	120.0	120.3	119.9
	2'''/6'''	109.3	109.2	109.3
	3'''/5'''	145.2	144.98	145.25
	4'''	138.4	138.1	138.5
Galloyl B	C=O	164.5	165.0	164.6
	1''''	119.9	120.5	119.85
	2''''/6''''	109.2	109.2	109.3
	3''''/5''''	145.0	145.0	145.0
	4''''	138.3	138.1	138.32
Galloyl C	C=O	164.9	165.5	164.9
	1''''	119.7		119.83
	2''''/6''''	109.2		109.1
	3''''/5''''	145.0		145.0
	4''''	138.2		138.3
	C=O	165.2		165.3

Recorded in ((CD₃)₂CO) at 100 MHz. Values in ppm (δ).

cellular leakage because they may diffuse through the bacterial cells' cytoplasmic membrane and thus increase the cells' permeability. The cellular leakage could be proteins, nucleic acids, and inorganic ions such as potassium or phosphates. Cell shrinkage and cell lysis were also observed in MRSA cells after exposure to the isolated compounds. This is because at a higher concentration, phenolic compounds might inhibit permease causing denaturation of the bacterial proteins. The disruption of cell membrane could subsequently cause cell shrinkage and cell lysis that may eventually lead to cell death (Maris, 1995). Phenolic compounds are also reported to inactivate intra-cytoplasmic enzymes by forming unstable complexes and causing the lipophilic molecules to be trapped by the membrane phospholipids. An increase in phenolic content will disrupt the equilibrium of surface macromolecules. This may affect the association of cell-surface polysaccharides and result in changes of bacterial shape and size (Dauang et al., 2011). This explains the changes in the size and shape of the MRSA cells after treatment with the compounds. The morphological features of the MRSA cells observed under the SEM indicates that compounds 1, 2, 3 and 6 had bactericidal effects on MRSA cells rather than a bacteriostatic one.

3. Concluding remarks

Eight flavonol rhamnosides, including three new galloylated flavonol rhamnosides, were isolated from the leaves of *C. tergemina*. This is the first report on the phytochemical study of *C. tergemina*. The anti-MRSA activity of the extracts and isolated flavonol

rhamnosides showed their structure–activity relationship where the esterification of the rhamnoside moiety was important in conferring anti-MRSA activity compared to the corresponding flavonol rhamnosides. There was no correlation between the degree of esterification and the antibacterial activity of these flavonol rhamnosides against MRSA. The lytic effect of the flavonol rhamnosides on MRSA were also confirmed by a scanning electron microscope imaging. Overall, the structure–activity-relationship of flavonol rhamnosides observed in this study could serve as a reference for the synthesis and design of new antimicrobial drugs.

4. Experimental

4.1. General

Silica gel (Kieselgel 60, 70–230, and 230–400 mesh, Merck KGaA, Darmstadt, Germany), and Sephadex LH-20 (Pharmacia Fine Chemicals AB, Uppsala, Sweden) were used for column chromatography (CC). Optical rotations were measured on an Atago AP-300 automatic polarimeter. Ultraviolet (UV) absorption spectra were measured in MeOH using a HPLC with a UV/VIS detector separated by a C-18 reversed phase column (Assentis 25 cm × 4.9 mm × 5 μm). The HPLC profiles were processed with Agilent software to obtain the UV λ_{max}. Nuclear magnetic resonance (NMR) spectra 1D and 2D were acquired on a Bruker-AVANCE-III operating at 400 MHz (¹H) and 100 MHz (¹³C). Mass spectra were carried out on a Q-TOF Mass Spectrometer (Agilent), in the negative ion mode of ionisation.

4.2. Plant material

Leaves of *C. tergemina* were collected in May 2011 from Klang Valley in Peninsular Malaysia and were identified by Anthonysamy Savarimuthu of the Plant Taxonomy Unit of School of Science, Monash University Sunway campus Malaysia where a voucher specimen (MUM-LEGUM-001) is deposited in the herbarium.

4.3. Extraction and Isolation

Freeze-dried *C. tergemina* leaves (1.5 kg) were extracted successively by adding 10 L each of hexane, CH₂Cl₂, EtOAc, MeOH and then H₂O at 25 °C for 3 days. The extracts were evaporated under reduced pressure. The EtOAc extract (40.0 g) was subjected to silica CC using an 80 mm column and eluted gradient-wise with mixtures of hexane–CHCl₃, CHCl₃–EtOAc and EtOAc–MeOH (2.5 L for each solvent mixture) to obtain 15 fractions of 500 ml each. Fraction 11 on evaporation to dryness yielded compound 8 (53.1 mg) while fraction 14 on treatment with EtOAc followed by MeOH gave compound 5 (35.2 mg) as a precipitate. 2.0 g of fraction 2 which showed the highest anti-MRSA activity was re-applied to a 40 mm silica column using 200 ml of the same solvent systems as above to obtain five sub-fractions. Sub-fractions 2–2 (311.0 mg), 2–3 (486.0 mg) and 2–4 (105.0 mg) also showed anti-MRSA activity and were separately subjected to gel filtration chromatography using Sephadex LH-20 eluting with MeOH. Sub-fraction 2–2–5 yielded compound 6 (34.3 mg), sub-fraction 2–2–7 gave compound 4 (15.9 mg), sub-fraction 2–2–9 yielded compound 7 (36.3 mg), sub-fraction 2–2–15 gave compound 2 (6.5 mg), and sub-fraction 2–2–17 on evaporation yielded compound 1 (18.2 mg). Sub-fraction 2–3–8 and 2–3–10 also yielded compound 1 (9.3 mg) and compound 3 (4.8 mg), respectively, after evaporation while sub-fraction 2–4–5 gave compound 3 (4.4 mg).

4.4. Analytical data

4.4.1. Kaempferol-3-O-(2'',3'',4''-tri-O-galloyl)- α -L-rhamnopyranoside (**1**)

Yellow amorphous powder; UV (MeOH) λ_{max} (nm): 212, 236, 275, 318, 340; $[\alpha]_{\text{D}}^{25} +25.3^{\circ}$ (c 0.1 in MeOH), for ^1H (400 MHz, $(\text{CD}_3)_2\text{CO}$) and ^{13}C (100 MHz, $(\text{CD}_3)_2\text{CO}$) NMR spectroscopic data, see Tables 3 and 4; Q-TOF MS m/z 887.1322 $[\text{M}-\text{H}]^-$ (calculated for $\text{C}_{42}\text{H}_{31}\text{O}_{22}$, 887.1307).

4.4.2. Quercetin-3-O-(3'',4''-di-O-galloyl)- α -L-rhamnopyranoside (**2**)

Yellow amorphous powder; UV (MeOH) λ_{max} (nm): 212, 228, 268, 350 nm; $[\alpha]_{\text{D}}^{25} +27.7^{\circ}$ (c 0.1 in MeOH), for ^1H (400 MHz, $(\text{CD}_3)_2\text{CO}$) and ^{13}C (100 MHz, $(\text{CD}_3)_2\text{CO}$) NMR spectroscopic data, see Tables 3 and 4; Q-TOF MS m/z 751.1156 $[\text{M}-\text{H}]^-$ (calculated for $\text{C}_{35}\text{H}_{27}\text{O}_{19}$, 751.1147).

4.4.3. Quercetin-3-O-(2'',3'',4''-tri-O-galloyl)- α -L-rhamnopyranoside (**3**)

Yellow amorphous powder; UV (MeOH) λ_{max} nm: 215, 260, 350 nm; $[\alpha]_{\text{D}}^{25} +27.3^{\circ}$ (c 0.1 in MeOH), for ^1H (400 MHz, $(\text{CD}_3)_2\text{CO}$) and ^{13}C (100 MHz, $(\text{CD}_3)_2\text{CO}$) NMR spectroscopic data, see Tables 3 and 4; Q-TOF MS m/z 903.1264 $[\text{M}-\text{H}]^-$ (calculated for $\text{C}_{42}\text{H}_{31}\text{O}_{23}$, 903.1256).

4.4.4. Acid hydrolysis

Compound **1** (7 mg) was hydrolysed with 1 M H_2SO_4 (2 ml) at room temperature overnight. The reaction mixture was then partitioned with EtOAc (3 mL). The aqueous layer was neutralised with 1.0 M $\text{Ba}(\text{OH})_2 \cdot 8\text{H}_2\text{O}$ (2 mL), filtered with glass wool and reduced under pressure to dryness. After treatment with EtOAc, MeOH and H_2O , L-rhamnose was obtained as white crystalline powder from the aqueous layer. The identity and purity of the sugar was confirmed by direct comparison (HPLC and TLC) with an authentic sample. The configuration of the rhamnose was determined to be L- $[\alpha]_{\text{D}}^{25} -7.8^{\circ}$ (c 0.6 in H_2O) (Hudson and Yanovsky, 1917; Lee et al., 2009): $[\alpha]_{\text{D}}^{25} -7.2^{\circ}$ (c 0.05 in H_2O).

4.5. Biological assay

4.5.1. Test microorganisms and media

All strains of MRSA used were sub-cultured from our laboratory stock culture collection, including clinical isolates of MRSA. Mueller-Hinton broth (MHB; Difco, MD, USA) were used for culturing the bacteria.

4.5.2. Antibacterial activity testing

4.5.2.1. Disc diffusion method. The anti-MRSA activities of the solvent crude extracts were tested using the disc diffusion method. The disc diffusion method was performed as described by Aksoy et al. (2006). The standardized bacterial inoculums were swabbed on the MHA agar plate using sterile cotton swab. When the agar surface was dried, 6.00 mm antimicrobial susceptibility discs containing the plant extract (1 mg/100 μl per disc) were placed aseptically on the agar using a needle. All samples were tested in triplicate. For positive control, a vancomycin antibiotic disc (30 μg /disc) was used while disc with MeOH was used as negative control. The agar plates were incubated at 37 $^{\circ}\text{C}$ for 16–20 h and the diameter of inhibition zone was measured and recorded. Crude extracts possessing antimicrobial activity were subjected to CC for the separation and isolation of the active compounds.

4.5.2.2. Microdilution method. Anti-MRSA activities of the isolated compounds were evaluated using the microdilution method as described by the Clinical and Laboratory Standards Institute (CLSI; Wiegand et al., 2008). The minimum inhibitory concentra-

tion (MIC) determinations were made in triplicate and vancomycin was used as positive control for the three strains of methicillin-resistant *S. aureus*, MRSA (ATCC: 33591), MRSA (Clinical Isolate 1) and MRSA (Clinical Isolate 2). Compounds were dissolved in 5% DMSO in H_2O . A serial two-fold dilution of the compounds was mixed with MHB in 96-well sterile microtitre plates to give a final concentration of 0.02–1.00 mg ml^{-1} . Inocula of 50 μl of the 24-h culture of each bacterial strain, containing approximately 5×10^5 CFU/ml, was applied into MHB supplemented with the tested compounds. MIC values were obtained after incubation at 37 $^{\circ}\text{C}$ for 24 h. The MICs were recorded as the lowest concentrations of tested compounds which completely inhibited bacterial growth.

4.5.3. Scanning Electron Microscope (SEM) analysis

After the MIC determination with microdilution, the bacterial cells from the 96 well plates with $2 \times$ MIC of the respective tested compounds, positive and negative controls were transferred separately into a centrifuge tube. The bacterial cells were spin down and washed thrice with phosphate buffer saline (PBS). On a glass slide, 20 μl of bacterial suspension was left to dry. The control and extract treated cells were fixed with 2.5% glutaraldehyde for 45 min and were later washed with PBS. The specimens were then dried with liq. N_2 and freeze dried. Using a splutter coater, the dried specimens were coated with a thin layer of platinum and were examined by a Scanning Electron Microscope.

Acknowledgements

The authors are thankful to Monash University Malaysia for financial support to EWLC for a visit to the Strathclyde Institute of Pharmacy and Biomedical Sciences, University of Strathclyde Glasgow for the use their NMR facilities and the University of Malaya Kuala Lumpur for LCMS analysis. We are grateful to Mr. Anthonysamy Savarimuthu (formerly of the University Putra Malaysia) for identifying the plant material.

Appendix A. Supplementary data

Supplementary data associated with this article can be found, in the online version, at <http://dx.doi.org/10.1016/j.phytochem.2014.07.028>.

References

- Agunu, A., Abdurahman, E.M., Shok, M., Yusuf, S.A., 2005. Analgesic activity of roots and leaves extracts of *Calliandra portoricensis*. *Fitoterapia* 76, 442–445.
- Aguwa, C.N., Lawal, A.M., 1988. Pharmacologic studies on the active principles of *Calliandra portoricensis* leaf extracts. *J. Ethnopharmacol.* 22, 63–71.
- Aksoy, A., Duran, N., Koksul, F., 2006. *In vitro* and *in vivo* antimicrobial effects of mastic chewing gum against *Streptococcus mutans* and *mutans streptococci*. *Arch. Oral. Biol.* 51 (6), 467–481.
- Chew, Y.L., Chan, W.L.E., Tan, P.L., Lim, Y.Y., Stanslas, J., Goh, J.K., 2011. Assessment of phytochemical content, polyphenolic composition, antioxidant and antibacterial activities of Leguminosae medicinal plants in Peninsular Malaysia. *BMC Complement Altern. Med.* <http://dx.doi.org/10.1186/1472-6882-11-12>.
- Cho, Y.S., Oh, J.J., Oh, K.H., 2010. Antimicrobial activity and biofilm formation inhibition of green tea polyphenols on human teeth. *Biotechnol. Bioprocess Eng.* 15, 359–364.
- Clinical and Laboratory Standards Institute (CLSI), 2002. Reference method for dilution antimicrobial susceptibility tests for bacteria that grow aerobically. Approved Standard, M7–A4. Clinical and Laboratory Standards Institute, Wayne, PA.
- Dauang, J., Vichitphan, S., Daduang, S., Hongsprabhas, P., Boonsiri, P., 2011. High phenolics and antioxidants of some tropical vegetables related to antibacterial and anticancer activities. *Afr. J. Pharm. Pharmacol.* 5 (5), 608–615.
- Eldahshan, O.A., 2011. Isolation and structure elucidation of phenolic compounds of carob leaves grown in Egypt. *Curr. Res. J. Biol. Sci.* 3, 52–55.
- Encarnacion, D.R., Ochoa, A.N., Anthoni, U., Christophersen, C., Nielsen, P.H., 1994. Two new flavones from *Calliandra californica*. *J. Nat. Prod.* 57, 1307.

- Hudson, C.S., Yanovsky, E., 1917. Indirect measurements of the rotatory powers of some alpha and beta forms of the sugars by means of solubility experiments. *J. Am. Chem. Soc.* 39, 1013–1037.
- Johnston, M.D., Hanlon, G.W., Denyer, S.P., Lambert, R.J.W., 2003. Membrane damage to bacteria caused by single and combined biocides. *J. Appl. Microbiol.* 94, 1015–1023.
- Lee, T.H., Chiang, Y.H., Chen, C.H., Chen, P.Y., Lee, C.K., 2009. A new flavonol galloylrhamnoside and a new lignan glucoside from the leaves of *Koelreuteria henryi* Dummer. *J. Nat. Med.* 63, 209–214.
- Mahmoud, I., Moharram, F.A., Marzouk, M.S., Soliman, H.S., el-Dib, R.A., 2001. Two new flavonol glycosides from leaves of *Koelreuteria paniculata*. *Pharmazie* 56, 580–582.
- Maris, P., 1995. Modes of action of disinfectants. *Rev. Sci. Tech.* 14, 47–55.
- Mattagajasingh, I., Acharya, L., Mukherjee, A.K., Panda, P.C., Das, P., 2006. Genetic relationships among nine cultivated taxa of *Calliandra* Benth. (Leguminosae: Mimosoideae) using random amplified polymorphic DNA (RAPD) markers. *Sci. Hortic.* 110, 98–103.
- Moharram, F.A., Marzouk, M.S.A., Ibrahim, M.T., Mabry, T.J., 2006. Antioxidant galloylated flavonol glycosides from *Calliandra haematocephala*. *Nat. Prod. Res.* 20, 927–934.
- Nohynek, L.J., Alakomi, H.L., Kahkonen, M.P., Heinonen, M., Helander, I.M., Oksman-Caldentey, K., Puupponen-Pimia, R.H., 2006. Berry phenolics: antimicrobial properties and mechanisms of action against severe human pathogens. *Nutr. Cancer* 54, 18–32.
- Orishadipe, A.T., Okogun, J.I., Mishelia, E., 2010. Gas chromatography – mass spectrometry analysis of the hexane extract of *Calliandra portoricensis* and its antimicrobial activity. *Afr. J. Pure Appl. Chem.* 4, 131–134.
- Otsuka, N., Liu, M.H., Shiota, S., Ogawa, W., Kuroda, T., Hatano, T., Tsuchiya, T., 2008. Anti-methicillin resistant *Staphylococcus aureus* (MRSA) compounds isolated from *Laurus nobilis*. *Biol. Pharm. Bull.* 31, 1794–1797.
- Sato, Y., Shibata, H., Arakaki, N., Higuti, T., 2004. 6,7-Dihydroxyflavone dramatically intensifies the susceptibility of methicillin-resistant or -sensitive *Staphylococcus aureus* to β -lactams. *Antimicrob. Agents Chemother.* 48, 1357–1360.
- Usia, T., Iwata, H., Hiratsuka, A., Watabe, T., Kodota, S., Tezuka, Y., 2004. Sesquiterpenes and flavonol glycosides from *Zingiber aromaticum* and their CYP3A4 and CYP2D6 inhibitory activities. *J. Nat. Prod.* 67, 1079–1083.
- Wiegand, I., Hilpert, K., Hancock, R.E.W., 2008. Agar and broth dilution methods to determine the minimal inhibitory concentration (MIC) of antimicrobial substances. *Nat. Protoc.* 3, 163–175.